

# Motion-Guided Dual-Camera Tracker for Low-Cost Skill Evaluation of Gastric Endoscopy

Yuelin Zhang<sup>1</sup>, Wanquan Yan<sup>1</sup>, Kim Yan<sup>1</sup>, Chun Ping Lam<sup>1</sup>, Yufu Qiu<sup>1</sup>,  
Pengyu Zheng<sup>1</sup>, Raymond Shing-Yan Tang<sup>2</sup>, Shing Shin Cheng<sup>1\*</sup>

<sup>1</sup>Department of Mechanical and Automation Engineering,  
The Chinese University of Hong Kong

<sup>2</sup>Department of Medicine and Therapeutics and Institute of Digestive Disease,  
The Chinese University of Hong Kong

**Abstract.** Gastric simulators with objective educational feedback have been proven useful for endoscopy training. Existing electronic simulators with feedback are however not commonly adopted due to their high cost. In this work, a motion-guided dual-camera tracker is proposed to provide reliable endoscope tip position feedback at a low cost inside a mechanical simulator for endoscopy skill evaluation, tackling several unique challenges. To address the issue of significant appearance variation of the endoscope tip while keeping dual-camera tracking consistency, the cross-camera mutual template strategy (CMT) is proposed to introduce dynamic transient mutual templates to dual-camera tracking. To alleviate disturbance from large occlusion and distortion by the light source from the endoscope tip, the Mamba-based motion-guided prediction head (MMH) is presented to aggregate visual tracking with historical motion information modeled by the state space model. The proposed tracker was evaluated on datasets captured by low-cost camera pairs during endoscopy procedures performed inside the mechanical simulator. The tracker achieves SOTA performance with robust and consistent tracking on dual cameras. Further downstream evaluation proves that the 3D tip position determined by the proposed tracker enables reliable skill differentiation. The code and dataset will be released upon acceptance.

**Keywords:** Object tracking · Dual-camera vision · Transformer · State space model · Endoscopy skill evaluation.

## 1 Introduction

Gastric endoscopy is a common clinical practice to allow thorough visual inspection of the upper gastric system via a flexible endoscope. A gastric endoscopist must undergo training before performing the procedure on patients. Existing endoscopy skill training and evaluation based on expert feedback has however raised concern for its lack of consistency and being susceptible to cognitive bias [1]. To avoid such bias, computerized or VR simulators with online feedback are

---

\* Corresponding author.

adopted [9]. However, their popularization is hindered due to the high cost of adoption [12]. Mechanical simulators have also been developed for endoscopy skill training, but do not provide educational feedback due to their simplicity in structure and the lack of sensor integration [9]. Providing gastric simulators with low-cost, yet objective educational feedback for effective skill evaluation during the endoscopy training stage thus remains an open research problem.

Endoscope motion tracking and analysis have been proven to be effective in surgical skill evaluation [17,23]. For example, electromagnetic tracker (EMT) has been attached to the endoscope to track its motion [25]. However, EMT is costly and can be affected by ferromagnetic materials. Its installation may also pose potential impairment to the endoscope tip flexibility. Vision-based tracking would be another approach to track the endoscope motion. One of the classical visual tracking structures is the Siamese tracker [19], which has been applied in many applications [4,6,33]. In recent years, trackers based on the transformer have been developed and achieved highly satisfactory performance [3,11,21]. Since a vision tracker has lower deployment cost, and does not need cumbersome setup and strict venue requirements like the EMT, it has been applied in many medical applications [2,32]. However, it has thus far not been applied for tracking a flexible endoscope in a mechanical gastric simulator (with vision trackers installed inside) intended for endoscopy skill evaluation. Tracking the tip of a flexible endoscope inside a realistic mechanical simulator involves many challenges, different from object tracking in natural scenes. The flexible endoscope tends to have a large workspace, resulting in **highly variable posture and appearance**, as well as **large occlusion**. Furthermore, the endoscope tip features an **intense light source which can cause severe distortion** to the image. These difficulties pose severe challenges to effective endoscope tracking.

During vision-based tracking of a surgical instrument, a multi-camera setup is usually adopted to estimate the 3D position of the target by dual-camera-based stereo matching [29] or multi-camera marker-based instrument tracking [30]. Although these multi-camera trackers report satisfactory performance, they are all evaluated using rigid markers or fiducial points under a stable environment. During tracking of the flexible endoscope tip in a mechanical simulator, the tracking system needs to adapt to its appearance change, where the target feature may become very different from the initial template. In this work, instead of using template updating or template-free strategy to adapt to feature variation [10,26], a **cross-camera mutual template strategy (CMT)** is proposed based on a dual-camera setup to make full use of mutual information from coupled cameras. CMT allows the tracking system to rely on not only the initial template but also the mutual template from synchronized frames in the coupled cameras. Tracking an object with a volatile appearance is then simplified by these dynamic transient mutual templates. CMT can also improve 3D tracking accuracy by introducing dual-camera tracking consistency.

The occlusion caused by endoscope posture variation and distortion caused by the light source at the endoscope tip calls for additional information beyond the direct visual features to help keep the target tracked. Historical motion informa-

tion has been proven to be helpful for robust tracking [21,22,31] by compensating for sudden target jumps and tracking loss. The existing works integrate motion sequence by fitting a probability model [31] or constructing high dimensional motion token [21], but fail to explore the long-range interrelationship within the time domain. Structured state space sequence models (SSMs) [18] draw considerable attention by their extraordinary long-range modeling ability, especially the Mamba [13,14], which introduces the selective scan mechanism to model long-range relationships in an input-dependent manner [24,28,35]. To fully explore the latent information from historical motion, the **Mamba-based motion-guided prediction head (MMH)** is proposed here to construct motion tokens from long-range temporal dependencies. This is the first time Mamba has been used for motion processing and medical instrument tracking.

In this work, a motion-guided dual-camera tracker is presented to enable endoscope tracking for endoscopy skill evaluation. The tracker achieves robust and accurate dual-camera tracking of the flexible endoscope tip under highly variable postures and a noisy environment (i.e. inside of a mechanical gastric simulator). The image dataset was self-collected by the dual-camera pairs installed inside a self-developed mechanical gastric simulator, and then labeled. The tracking is tested in both 2D and 3D metrics. The proposed method outperforms all state-of-the-art methods and evaluation in downstream tasks proves its validity for endoscopy skill evaluation. The contributions are three folds: 1) The dual-camera-based cross-camera mutual template strategy (CMT) is proposed to adapt to the variable appearance of the endoscope tip while enhancing dual-camera tracking consistency by performing tracking on dynamic transient mutual templates; 2) The Mamba-based motion-guided prediction head (MMH) is proposed to integrate historical motion, achieving consistent and robust tracking even when the target disappears under strong distortion; 3) The proposed tracker has low reliance on hardware specifications. Low-cost cameras (approx. 15 USD) can be installed in existing mechanical simulators to provide robust vision-based tracking for reliable skill evaluation during endoscopy training.

## 2 Method

### 2.1 Overview

As shown in Fig. 1, the tracker receives two search maps  $x_1$  and  $x_2$  from dual cameras and a template map  $z$  (from camera 1 by default), and extracts features with Siamese ResNet [16] backbone following similar workflow with existing Siamese trackers [5,21]. The CMT modules are placed after backbone stages  $\varphi_n$  ( $n \in \{3, 4, 5\}$ ), before prediction heads. It aggregates features from the coupled camera into the original template  $\varphi_n(z)$ , generating mutual templates  $\omega_1^n$  and  $\omega_2^n$  for  $\varphi_n(x_1)$  and  $\varphi_n(x_2)$ , respectively. In the following MMH, the concatenated  $[\omega_i^n, \varphi_n(x_i)]$  goes through multi-head self-attention [27], and then goes into vision-motion integrator to integrate historical motion from Mamba bidirectional motion tokenizer. The classification map and regression map of image

$x_i$  are then predicted by convolution layers. After 2D tracking results (bounding boxes) on  $x_1$  and  $x_2$  are predicted, the 3D position is estimated based on dual-camera stereo disparity [15].

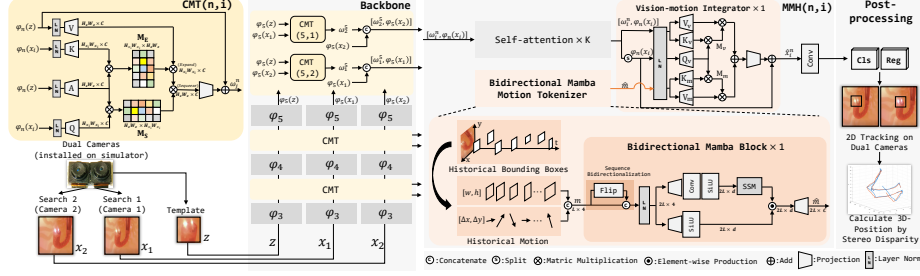


**Fig. 1.** Structure overview.  $\varphi_n$  denote the layers in the Siamese ResNet [16] backbone, where  $n \in \{3, 4, 5\}$ . For simplicity, the figure only shows  $CMT(n, i)$  and  $MMH(n, i)$  for  $\varphi_n(x_i)$  ( $\{i, j\} = \{1, 2\}$ ). All  $\varphi_n(x_i)$  follow the same workflow.

## 2.2 Cross-camera Mutual Template Strategy (CMT)

Since the flexible endoscope tip has highly variable posture and appearance, the original template from the initial frame may not be informative for all frames along the whole procedure. Furthermore, the tracking consistency between dual cameras is important for the accuracy of stereo disparity and 3D position [15]. By assuming the transient features from dual cameras have high consistency, CMT generates mutual templates dynamically for each camera by aggregating the synchronized frames from coupled cameras, as shown in Fig. 1. CMT relies on the proposed **anchored expansion-squeeze cross-attention**, given by:

$$M_E = \text{Softmax}(\mathbf{K}(\text{LN}(\varphi_n(x_i))) \cdot \mathbf{A}(\text{LN}(\varphi_n(z)))^T / \sqrt{C}), \quad (1)$$

$$M_S = \text{Softmax}(\mathbf{A}(\text{LN}(\varphi_n(z))) \cdot \mathbf{Q}(\text{LN}(\varphi_n(x_i)))^T / \sqrt{C}), \quad (2)$$

$$\omega_j^n = \text{Linear}(M_S \cdot (M_E \cdot \mathbf{V}(\text{LN}(\varphi_n(z)))) + \varphi_n(z), \quad (3)$$

where  $\text{LN}(\cdot)$  refers to layer normalization,  $C$  denotes the embedded dimension ( $C = 256$  in this paper), and  $\{i, j\} = \{1, 2\}$ .  $\mathbf{A}(\cdot)$  is an additional anchor projection besides the standard  $\mathbf{Q}(\cdot)$ ,  $\mathbf{K}(\cdot)$ ,  $\mathbf{V}(\cdot)$  projections. By applying  $\mathbf{A}(\cdot)$  as an intermediate transformation between  $\varphi_n(z) \in \mathbb{R}^{C \times H_z W_z}$  and  $\varphi_n(x_i) \in \mathbb{R}^{C \times H_{x_i} W_{x_i}}$ , the expansion attention map  $M_E \in \mathbb{R}^{H_{x_i} W_{x_i} \times H_z W_z}$  and squeeze attention map  $M_S \in \mathbb{R}^{H_z W_z \times H_{x_i} W_{x_i}}$  are obtained. The anchored expansion-squeeze operation is performed by multiplying  $\mathbf{V}$  with  $M_E$  and  $M_S$  successively, where  $\mathbf{V}$  is expanded into larger embedded space with richer representation and then squeezed back to its original size. This expansion and squeeze workflow enables modeling positional attention between maps with different sizes while enlarging the intermediate projection space. The obtained mutual template  $\omega_j^n$  is then concatenated with  $\varphi_n(x_j)$  for tracking prediction.

With CMT, the two feature maps from dual cameras become mutual templates of each other. They are dynamically aggregated within a transient period to guarantee the template timeliness and informativeness, addressing the appearance variation problem and ensuring dual-camera tracking consistency.

### 2.3 Mamba-based Motion-guided Prediction Head (MMH)

The MMH receives search map  $\varphi_n(x_i)$  and its mutual template  $\omega_i^n$ . As shown in Fig. 1, the concatenated input map  $[\omega_i^n, \varphi_n(x_i)]$  is first processed by  $K$  cascaded multi-head self-attention modules [27] ( $K = 6$ ). To construct the motion token, instead of directly projecting coordinates of bounding box [21], in this paper, the historical bounding boxes are first converted from absolute position in the image coordinate system to relative descriptors in the bounding box coordinate system. This conversion enhances generalizability by replacing absolute value with relative local parameters. The obtained low-level local descriptors contain box width and height  $(w, h)$  and displacement in  $x$  axis and  $y$  axis  $(\Delta x, \Delta y)$  along the time domain. They are then concatenated together to learn the latent internal relationship between the box size and the displacement.

The following **bidirectional Mamba block** models the long-range dependencies along time. Since Mamba modeling is unidirectional, the bidirectionalization is first performed as shown in Fig. 1 to expand the raw sequence  $m \in \mathbb{R}^{L \times 4}$  into bidirectional form with a size of  $2L \times 4$ . After a layer normalization, the input sequence goes through projection, convolution, and SiLU activation [8] in two branches to get the embedded maps with a size of  $2L \times d$ , where  $d = 128$  in this paper. SSM is defined by linear Ordinary Differential Equations (ODEs) given by  $h'(t) = \mathbf{A}h(t) + \mathbf{B}x(t)$ ,  $y(t) = \mathbf{C}h(t)$ , where  $\mathbf{A} \in \mathbb{R}^{N \times N}$  is the state matrix,  $\mathbf{B} \in \mathbb{R}^{N \times 1}$  and  $\mathbf{C} \in \mathbb{R}^{N \times 1}$  are projection matrices. It maps the input sequence  $x(t) \in \mathbb{R}^N$  to output  $y(t) \in \mathbb{R}^N$  with latent states  $h(t) \in \mathbb{R}^N$ . These linear ODEs are then discretized as  $h_t = \bar{\mathbf{A}}h_{t-1} + \bar{\mathbf{B}}x_t$ ,  $y_t = \bar{\mathbf{C}}h_t$ . The discretized matrices  $\bar{\mathbf{A}}$  and  $\bar{\mathbf{B}}$  are given by  $\bar{\mathbf{A}} = \exp(\Delta \cdot \mathbf{A})$  and  $\bar{\mathbf{B}} = (\Delta \cdot \mathbf{A})^{-1}(\exp(\Delta \cdot \mathbf{A}) - \mathbf{I}) \cdot (\Delta \mathbf{B})$ , where  $\Delta$  is the discretization step size. Here selective scan SSM [13] is adopted. It improves the traditional SSMs by parameterizing the SSM based on input, where the parameters  $\Delta, \mathbf{B}, \mathbf{C}$  are obtained from projections of the input sequence. After SSM, the output is then element-wise multiplied with the other branch. Finally, the embedded maps are projected into bidirectional motion token  $\hat{m} \in \mathbb{R}^{2L \times C}$ .

The motion token  $\hat{m}$  is then integrated with the vision feature using the proposed **vision-motion integrator**, which is a multi- $KV$  cross-attention as shown in Fig. 1. This operation is given by:

$$M_v = \text{Softmax}(\mathbf{Q}_v(\text{LN}(\varphi_n(x_i))) \cdot \mathbf{K}_v(\text{LN}([\omega_i^n, \varphi_n(x_i)]))^T / \sqrt{C}), \quad (4)$$

$$M_m = \text{Softmax}(\mathbf{Q}_v(\text{LN}(\varphi_n(x_i))) \cdot \mathbf{K}_m(\text{LN}(\hat{m}))^T / \sqrt{C}), \quad (5)$$

$$\hat{x}_i^n = \text{Linear}(M_v \cdot \mathbf{V}_v(\text{LN}([\omega_i^n, \varphi_n(x_i)])) + M_m \cdot \mathbf{V}_m(\hat{m}) + \varphi_n(x_i), \quad (6)$$

where  $M_v$  and  $M_m$  are attention maps for visual feature and motion hints, respectively. By applying this operation, the vision feature map is losslessly

integrated with the historical motion hints, without losing the self-contained positional embedding. Finally, classification and regression are performed on  $\hat{x}_i^n$  using convolution to obtain the 2D tracking result on  $x_i$ .

With MMH, the historical motion is tokenized by the Mamba tokenizer and introduced as non-visual hints for robust tracking. It is especially helpful when the target is temporarily lost due to occlusion or light disturbance.

### 3 Experiments and Results

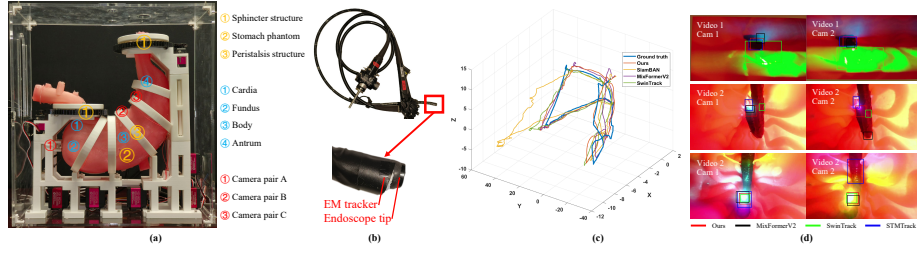


**Fig. 2.** Experimental setup and result demonstrations. (a) Self-developed mechanical gastric simulator and installation of dual-camera tracking devices. (b) Flexible gastric endoscope with EMT affixed at its tip to provide the 3D ground truth. (c)-(d) Estimated 3D motion of the endoscope tip and snapshots of the tracking performance by state-of-the-art trackers, including the proposed tracker.

#### 3.1 Experiment Setup and Dataset

As shown in Fig. 2(a), a customized mechanical gastric simulator was developed as a realistic simulating platform for endoscopy training. The salmon-color, highly distensible silicone stomach phantom has a thin wall and two openings with sphincters. It has a sphincter movement structure and a peristalsis actuation structure to simulate the dynamic behavior of the human stomach. Three pairs of calibrated binocular cameras (Fig. 2(a)) were installed on the inside of the phantom wall, where pair A was at the fundus region, and pair B and C were on the lesser curvature of the stomach body. Note that such dual-camera pairs can be constructed at a very low cost using cheap cameras (approx. 15 USD).

An Olympus GIF-FQ260Z endoscope was manipulated inside the simulator during the experiments. A dataset with 14530 images of the endoscope at different postures was collected and divided into training and testing sets with 10270 and 4260 images. The bounding boxes of the endoscope tip were annotated on original images as 2D ground truth by only one annotator to eliminate disagreement and bias. The 3D position ground truth was measured by an EMT affixed on the endoscope tip (Fig. 2(b)). The program was implemented with PyTorch. The proposed tracker and all comparison methods were trained on the collected dataset by four NVIDIA RTX 4090 GPUs (batch size 24, 150 epochs).

**Table 1.** Endoscope tracking comparison and ablation study results.

Method	2D Metrics (%)		3D Metrics (mm)		
	SUC $\uparrow$	PRE $\uparrow$	Avg err. $\downarrow$	Max err. $\downarrow$	SD $\downarrow$
SiamRPN++ [20]	60.1	59.7	7.93	370.48	13.49
SiamBAN [5]	67.0	67.8	7.58	248.79	12.51
SiamAttn [34]	67.5	66.3	11.12	85.06	7.91
STMTrack [10]	70.0	69.4	9.56	69.82	8.51
SwinTrack [21]	75.2	74.6	10.82	57.81	7.67
MixFormerV2 [7]	77.8	77.1	7.68	49.38	9.53
<b>Ours</b>	<b>79.6</b>	<b>79.8</b>	<b>4.97</b>	<b>14.34</b>	<b>3.68</b>
Ablation Study					
baseline	72.4	70.5	11.09	158.30	10.36
w/ MMH, w/o CMT	76.6	77.2	9.28	60.74	6.92
w/ CMT, w/o MMH	78.5	79.0	6.89	20.53	7.90
SwinTrack [21] + CMT	75.9	74.8	8.62	39.90	6.21

### 3.2 Results and Discussion

The proposed tracker is compared against several state-of-the-art trackers, as shown in Tab. 1, including the latest transformer-based tracker [7], tracker with motion token [21], classical Siamese tracker [20], etc. All methods first perform 2D tracking on each image of dual cameras and estimate 3D position using stereo disparity. The result of the 2D evaluation is given by the success rate (SUC) with an overlap threshold of 0.5 and precision (PRE) with a location error threshold of 20 pixels. The results show the proposed tracker achieves SOTA performance with 79.6 SUC and 79.8 PRE. Tracking comparison given in Fig. 2(d) shows that our method achieves more accurate and robust tracking against light disturbance, occlusion, and appearance variation. More tracking demonstration is provided in the supplementary video. For evaluation of 3D tracking, three metrics are used, including average error, maximum error, and standard deviation (SD). Our tracker outperforms the other methods significantly in all three metrics, achieving 35%, 71%, and 61% improvement respectively against the second-best method. The demonstration shown in Fig. 2(c) also shows that the 3D trajectory obtained from our tracker has less noise and error.

During the ablation study, the baseline model removes CMT and Mamba motion tokenizer, where the MMH is then degraded into a commonly used transformer head with self-attention and cross-attention. As shown in Tab. 1, the model with MMH or CMT has significant improvement over the baseline in both 2D and 3D metrics. Integrating MMH allows the maximum error and SD to be reduced by 62% and 33%, proving the integrated historical motion token can help the tracker avoid large errors due to target disappearance, leading to more robust tracking. Integrating CMT allows the accuracy of 2D tracking and 3D position estimation to be significantly improved, especially with a reduction in the maximum 3D error. It shows that CMT keeps accurate and robust tracking during the whole procedure, leveraging the dual-camera mutual templates.

Additional test was performed by applying CMT on SwinTrack [21], which has similar Siamese backbone and transformer head. Improvement is observed in all metrics, proving the generalizability of the proposed CMT.

Compared with STMTrack [10] which adopts a template-free strategy by using embedded features of historical frames as template, the mutual template strategy applied in CMT uses transient features from coupled cameras as template to guarantee the timeliness and informativeness while avoiding error accumulation, thus outperforming STMTrack. SwinTrack [21] also adopts a learnable motion tokenizer, but it fails to extract lower-level motion descriptors to eliminate absolute information and does not apply sequence modeling module to model time-domain dependencies, resulting in less benefit from motion information. The proposed tracker achieves SOTA in both 2D and 3D evaluations. According to Tab. 1, the improvement in 3D metrics is much more significant than in 2D metrics. The reason is that the proposed CMT can not only tackle appearance variation problem by dynamic transient mutual templates but also introduce binocular visual constraints into dual-camera tracking, thus ensuring tracking consistency between two cameras. This improvement greatly improves the accuracy of 3D position estimation that relies on stereo disparity.

**Table 2.** Skill evaluation according to motion metrics [23]. The statistical significance ( $p$  value) is given by a Mann-Whitney  $U$ -test, where significant differences at the  $p \leq 0.05$  level are indicated in bold.

	T (s)	IT (%)	PL (m)	S (mm/s)	A (mm/s <sup>2</sup> )	MS (mm/s <sup>3</sup> )	EOV (-)
expert	125	18.41	8.09	31.17	12.49	13.41	0.0056
novice	217	10.28	27.74	46.32	15.90	15.12	0.0036
$p$ value	<b>0.003</b>	<b>0.011</b>	<b>0.003</b>	<b>0.003</b>	<b>0.005</b>	0.25	<b>0.029</b>

**Skill Evaluation Tests** Skill evaluation tests were conducted by inviting expert and novice surgeons (expertise defined based on ASGE standards) to perform a series of endoscopy procedures in the gastric simulator (see appendix for details). A total of 15 trials by three experts (more than 1000 endoscopy cases performed) and 36 trials by six novices (less than 130 endoscopy cases performed) are included. The 3D motion trajectories of the endoscope tip were acquired by the proposed tracker. The skill evaluation is then given by analyzing motion metrics [23], including T (time), IT (idle time percentage), PL (average path length), S (average speed), A (average acceleration), MS (motion smoothness), and EOv (economy of volume). The result is shown in Tab. 2. To confirm the statistical significance of the skill evaluation results and prove the results acquired by the proposed tracker can clearly differentiate between experts and novices, a Mann-Whitney  $U$ -test is performed and the statistical significance is given by the  $p$  value, as shown in Tab. 2. Statistical significance ( $p \leq 0.05$ ) was found in 6 out of 7 metrics, confirming our tracker’s feasibility for skill evaluation.



## 4 Conclusion

In this paper, a motion-guided dual-camera tracker with CMT and MMH module is proposed for vision-based tracking of the endoscope tip inside a mechanical gastric simulator to allow endoscopy skill evaluation during endoscopy training. The tracker achieves SOTA performance in 2D and 3D tests, enabling reliable and accurate 3D tip position feedback. In the future, skill evaluations involving a larger cohort will be conducted to further validate the effectiveness of the proposed tracker.

## References

1. Anderson, M.J., et al.: Techniques in gastrointestinal endoscopy: surgical endoscopy. *Techniques in Gastrointestinal Endoscopy* **20**(4), 162–165 (2018)
2. Bouget, D., et al.: Vision-based and marker-less surgical tool detection and tracking: a review of the literature. *Medical image analysis* **35**, 633–654 (2017)
3. Chen, X., et al.: Transformer tracking. In: *Proceedings of the IEEE/CVF conference on computer vision and pattern recognition*. pp. 8126–8135 (2021)
4. Chen, Z., et al.: Siamese box adaptive network for visual tracking. In: *Proceedings of the IEEE/CVF conference on computer vision and pattern recognition*. pp. 6668–6677 (2020)
5. Chen, Z., et al.: Siamban: target-aware tracking with siamese box adaptive network. *IEEE Transactions on Pattern Analysis and Machine Intelligence* (2022)
6. Cheng, S., et al.: Learning to filter: Siamese relation network for robust tracking. In: *Proceedings of the IEEE/CVF conference on computer vision and pattern recognition*. pp. 4421–4431 (2021)
7. Cui, Y., et al.: Mixformerv2: Efficient fully transformer tracking. *Advances in Neural Information Processing Systems* **36** (2024)
8. Elfwing, S., et al.: Sigmoid-weighted linear units for neural network function approximation in reinforcement learning. *Neural networks* **107**, 3–11 (2018)
9. Finocchiaro, M., et al.: Training simulators for gastrointestinal endoscopy: current and future perspectives. *Cancers* **13**(6), 1427 (2021)
10. Fu, Z., et al.: Stmtrack: Template-free visual tracking with space-time memory networks. In: *Proceedings of the IEEE/CVF Conference on Computer Vision and Pattern Recognition*. pp. 13774–13783 (2021)
11. Gao, S., et al.: Generalized relation modeling for transformer tracking. In: *Proceedings of the IEEE/CVF Conference on Computer Vision and Pattern Recognition*. pp. 18686–18695 (2023)
12. Goodman, A.J., et al.: Endoscopic simulators. *Gastrointestinal Endoscopy* **90**(1), 1–12 (2019)
13. Gu, A., Dao, T.: Mamba: Linear-time sequence modeling with selective state spaces. *arXiv preprint arXiv:2312.00752* (2023)
14. Gu, A., et al.: Combining recurrent, convolutional, and continuous-time models with linear state space layers. *Advances in neural information processing systems* **34**, 572–585 (2021)
15. Hamzah, R.A., et al.: Literature survey on stereo vision disparity map algorithms. *Journal of Sensors* **2016** (2016)
16. He, K., et al.: Deep residual learning for image recognition. In: *Proceedings of the IEEE conference on computer vision and pattern recognition*. pp. 770–778 (2016)

17. Islam, G., Kahol, K.: Application of computer vision algorithm in surgical skill assessment. In: 7th International Conference on Broadband Communications and Biomedical Applications. pp. 108–111. IEEE (2011)
18. Kalman, R.E.: A new approach to linear filtering and prediction problems (1960)
19. Li, B., et al.: Siamrpn++: Evolution of siamese visual tracking with very deep networks. In: Proceedings of the IEEE/CVF conference on computer vision and pattern recognition. pp. 4282–4291 (2019)
20. Li, B., et al.: Siamrpn++: Evolution of siamese visual tracking with very deep networks. In: Proceedings of the IEEE/CVF conference on computer vision and pattern recognition. pp. 4282–4291 (2019)
21. Lin, L., et al.: Swintrack: A simple and strong baseline for transformer tracking. *Advances in Neural Information Processing Systems* **35**, 16743–16754 (2022)
22. Mwikirize, C., et al.: Time-aware deep neural networks for needle tip localization in 2d ultrasound. *International Journal of Computer Assisted Radiology and Surgery* **16**, 819–827 (2021)
23. Oropesa, I., et al.: Eva: laparoscopic instrument tracking based on endoscopic video analysis for psychomotor skills assessment. *Surgical endoscopy* **27**, 1029–1039 (2013)
24. Ruan, J., et al.: Vm-unet: Vision mamba unet for medical image segmentation. arXiv preprint arXiv:2402.02491 (2024)
25. Safavian, N., et al.: Endoscopic measurement of the size of gastrointestinal polyps using an electromagnetic tracking system and computer vision-based algorithm. *International Journal of Computer Assisted Radiology and Surgery* pp. 1–9 (2023)
26. Sun, M., et al.: Fast template matching and update for video object tracking and segmentation. In: Proceedings of the IEEE/CVF Conference on Computer Vision and Pattern Recognition. pp. 10791–10799 (2020)
27. Vaswani, A., et al.: Attention is all you need. *Advances in neural information processing systems* **30** (2017)
28. Wang, C., et al.: Graph-mamba: Towards long-range graph sequence modeling with selective state spaces. arXiv preprint arXiv:2402.00789 (2024)
29. Wang, C., et al.: Stereo video analysis for instrument tracking in image-guided surgery. In: 2014 5th European Workshop on Visual Information Processing (EU-VIP). pp. 1–6. IEEE (2014)
30. Wang, J., et al.: Surgical instrument tracking by multiple monocular modules and a sensor fusion approach. *IEEE Transactions on Automation Science and Engineering* **16**(2), 629–639 (2018)
31. Yan, W., et al.: Learning-based needle tip tracking in 2d ultrasound by fusing visual tracking and motion prediction. *Medical Image Analysis* **88**, 102847 (2023)
32. Yang, C., et al.: Image-based laparoscopic tool detection and tracking using convolutional neural networks: a review of the literature. *Computer Assisted Surgery* **25**(1), 15–28 (2020)
33. Yang, Z., et al.: Siammmf: multi-modal multi-level fusion object tracking based on siamese networks. *Machine Vision and Applications* **34**(1), 7 (2023)
34. Yu, Y., et al.: Deformable siamese attention networks for visual object tracking. In: Proceedings of the IEEE/CVF conference on computer vision and pattern recognition. pp. 6728–6737 (2020)
35. Zhu, L., et al.: Vision mamba: Efficient visual representation learning with bidirectional state space model. arXiv preprint arXiv:2401.09417 (2024)